Final Report of NASA Contract # NAG9-838 entitled "Compact laser multi-gas spectral sensors for spacecraft systems"

Period: September 1, 1995–February 28, 1997

Principal Investigator: Frank K. Tittel

Department of Electrical and Computer Engineering

Rice University

P.O. Box 1892, MS 366

Houston, TX 77251-1892

(713) 527-4833 (Telephone)

(713) 524-5237 (Fax)

fkt@rice.edu (Email)

Project Objectives:

The objective of this research effort has been the development of a new gas sensor technology to meet NASA requirements for spacecraft and space station human life support systems for sensitive selective and real time detection of trace gas species in the mid-infrared spectral region.

Project Approach:

The gas sensor technology makes use of difference frequency mixing of diode lasers or diode laser pumped solid state lasers in nonlinear optical materials.

Accomplishments:

The work has led to the development and performance evaluation of several gas sensor schemes:

(1) Detection of methane in air of 12 ppb $(Hz)^{-1/2}$ near 3.2 μm. This source uses $AgGaS_2$ as the nonlinear medium pumped by a compact 1064 nm Nd:YAG laser and a diode laser operating near 800 mn.

(2) Detection of CO, N_2O, and CO_2 in ambient air based on DFG in periodically poled $LiNbO_3$ (PPLN). The CO detection sensitivity is extrapolated to 5 ppb·m/$\sqrt{Hz}$ if limited by IR intensity noise.

(3) Development of a cw tunable 8.7 μm spectroscopic source based on fiber coupled DFG in $AgGaSe_2$. The DFG source was applied to monitor SO_2 concentration levels.

(4) Study of a log wavelength CW IR source based on DFG in gallium selenide ($GaSe$). A long wavelength cw IR source continuously tunable in the 8.8-15 micron wavelength region was demonstrated. Detection of ethylene was demonstrated successfully near 945 cm^{-1}.

Publications:

1. U. Simon and F.K. Tittel, "Recent Progress in Tunable Nonlinear Optical Devices for Infrared Spectroscopy," *Infrared Phys. Technol.* **36**, 427-438 (1995).

2. K. Petrov, S. Waltman, R. Curl, F. Tittel, and L. Hollberg, "Detection of Methane in Air using Diode-Laser-Pumped Difference-Frequency Generation near 3.2 μm," *Appl. Phys. B* **61**, 553-558 (1995).

3. K.P. Petrov, L. Goldberg, W.K. Burns, R.F. Curl, and F.K. Tittel, "Detection of CO in Air Using Diode-Pumped 4.6 μm Difference Frequency Generation in Quasi-Phase-Matched $LiNbO_3$," *Optics Letters* **21**, 86-88 (1996).

4. K.P. Petrov, R.F. Curl, F.K. Tittel, and L. Goldberg, "CW tunable 8.7-μm spectroscopic source pumped by fiber-coupled communications lasers," *Optics Letters* **21**, 1451-1453 (1996).

5. Wade C. Eckhoff, Roger S. Putnam, Shunxi Wang, Robert F. Curl, and Frank K. Tittel, "A Continuously Tunable Long Wavelength CW IR Source for High-Resolution Spectroscopy and Trace Gas Detection," *Applied Physics B* **63**, 437 (1996).

Presentations:

1. "Tunable Infrared Laser Sources for Spectroscopy and Atmospheric Trace Gas Detection," F.K. Tittel, D.P. Petrov, S. Waltman, L. Hollberg, and R.F. Curl, 12th Int'l Conf. on Laser Spectroscopy, Capri, Italy (June 11-16, 1995).

2. "Compact Tunable Mid-Infrared Laser Sources: Technology and Applications," F.K. Tittel, K. Petrov, U. Simon, and R.F. Curl, Laser Optics '95, St. Petersburg (June 27-July 1, 1995).

3. "Tunable Infrared Source by Difference Frequency Mixing Diode Lasers and Diode-Pumped YAG, and Application to Methane Detection," S. Waltman, L. Hollberg,

K. Petrov, U. Simon, F. Tittel, and R. Curl, Semiconductor Lasers: Advanced Devices and Applications, Keystone, CO (Aug. 21-23, 1995).

4. "CO Trace Detection in Air using Diode-Pumped Quasiphasematched CW Difference Frequency Generation," Konstantin Petrov, L Goldberg, W.K. Burns, R.F. Curl, and Frank K. Tittel, 1995 Center for Nonlinear Optical Materials Affiliates Meeting, Stanford, CA (Sept. 20, 1995).

5. "Tunable Diode Laser Based Mid-Infrared Sources for Spectroscopy," K.P. Petrov, R.F. Curl, and F.K. Tittel, Am. Phys. Soc. Texas Section Mtg., Lubbock, TX (Oct. 27-29, 1995).

6. "Application of a Diode-Laser-Based CW Tunable IR Source to Methane Detection in Air," K.P. Petrov, S. Waltman, R.F. Curl, F.K. Tittel, and L. Hollberg, IEEE LEOS 1995 Ann. Mtg., San Francisco, CA (Oct. 30-Nov. 2, 1995).

7. "Recent Advances in Tunable Mid-Infrared Laser Sources for Environmental Gas Monitoring," F.K. Tittel, K.P. Petrov, R.F. Curl, L. Goldberg, W.K. Burns, S. Waltman, E.J. Dlugokencky, and L.W. Hollberg, 16th Annual Meeting of Laser Society of Japan, Yokohama, Japan (Jan. 24-25, 1996).

8. "Detection of Spacecraft Cabin Air Contaminants Using Infrared Laser-Based Methods," K.P. Petrov, L. Goldberg, S. Waltman, W.K. Burns, L.W. Hollberg, E.J. Dlugokencky, R.F. Curl, and F.K. Tittel, NASA/AIAA Life Sciences & Space Medicine Conf. (March 5-7, 1996).

9. "Recent Developments of All-Solid-State Mid-Infrared Sources for Spectroscopy and Environmental Applications," F.K. Tittel, K.P. Petrov, and R.F. Curl, German Physical Society Meeting, Jena, Germany (March 11-15, 1996).

10. "Extending Wavelength Coverage and Spectroscopic Applications," R.W. Fox, L. Hollberg, S. Waltman, K.P. Petrov, and F.K. Tittel, OSA Top. Meeting on Laser applications to Chemical and Environmental Analysis, Orlando, FL (March 20-22, 1996).

11. "Diode-Pumped Quasi-Phase-Matched CW 4.6 μm Source: Application to Trace Gas Detection," K.P. Petrov, R.F. Curl, F.K. Tittel, L. Goldberg, and W.K. Burns, CLEO '96, Anaheim, CA (June 2-7, 1996).

12. "A Continuously Tunable Long Wavelength CW DFG IR Source Suitable for High-Resolution Spectroscopy and Trace Gas Detection," Wade C. Eckhoff, Shunxi Wang, Robert F. Curl, Frank K. Tittel, and Roger Putnam, CLEO '96, Anaheim, CA (June 2-7, 1996).

13. "Infrared Sources for Spectroscopy Based on Difference Frequency Generation," F.K. Tittel, R.F. Curl, K.P. Petrov, W.C. Eckhoff, Sh. Wang, R.S. Putnam, L. Hollberg, S. Waltman, L. Goldberg, and W.K. Burns, 51st Int'l Ohio State Conf. on Molecular Spectroscopy (June 20-23, 1996).

14. "Applications of Lasers in Environmental Sensing," F.K. Tittel, K.P. Petrov, and R.F. Curl, IQEC '96, Sydney, Australia (July 14-19, 1996).

15. "Precise Measurement of CH_4 in Natural Air Using Diode-Pumped 3.4 μm Difference-Frequency Source," K.P. Petrov, S. Waltman, E.J. Dlugokencky, M. Arbore, M.M. Fejer, F.K. Tittel, and L.W. Hollberg, 1996 Center for Nonlinear Optical Materials Affiliates Meeting, Stanford University, Stanford, CA (Sept. 17-18, 1996).

16. "Compact Mid-Infrared Laser Based Sensor Technology for Trace Gas Detection," F.K. Tittel, NASA Advanced Technologies Workshop, Houston, TX (Sept. 25-27, 1996).

Appl. Phys. B 61, 553–558 (1995)

Applied Physics B Lasers and Optics

Detection of methane in air using diode-laser pumped difference-frequency generation near 3.2 μm

K. P. Petrov[1], S. Waltman[2], U. Simon[1], R. F. Curl[1], F. K. Tittel[1], E. J. Dlugokencky[3], L. Hollberg[2]

[1] Departments of Electrical and Computer Engineering, and Chemistry, Rice University, Houston, TX 77251-1892, USA
(Fax: + 1-713/524-5237, E-mail: FKT@rice.edu)
[2] Time and Frequency Division, National Institute of Standards and Technology, 325 Broadway, Boulder, CO 80303, USA
[3] National Oceanic and Atmospheric Administration, 325 Broadway, Boulder, CO 80303, USA

Received: 23 June 1995/Accepted: 1 July 1995

Abstract. Spectroscopic detection of the methane in natural air using an 800 nm diode laser and a diode-pumped 1064 nm Nd:YAG laser to produce tunable light near 3.2 μm is reported. The lasers were pump sources for ring-cavity-enhanced tunable difference-frequency mixing in $AgGaS_2$. IR frequency tuning between 3076 and 3183 cm^{-1} was performed by crystal rotation and tuning of the extended-cavity diode laser. Feedback stabilization of the IR power reduced intensity noise below the detector noise level. Direct absorption and wavelength-modulation ($2f$) spectroscopy of the methane in natural air at 10.7 kPa (80 torr) were performed in a 1 m single-pass cell with 1 μW probe power. Methane has also been detected using a 3.2 μm confocal build-up cavity in conjunction with an intracavity absorption cell. The best methane detection limit observed was 12 ppb m $(Hz.)^{-1/2}$.

PACS: 07.65; 33.00; 42.60; 42.65; 42.80

This work was done to develop a diode-laser-based technique for sensitive detection of environmentally important atmospheric trace gases such as methane, carbon monoxide, nitrous oxide, and nitric oxide. Several measurements of optical absorption in methane using tunable near-infrared lasers have been reported recently. Lucchesini et al. have used diode lasers to access $3\nu_1 + \nu_3 + (\nu_2$ or $\nu_4)$ combination-overtone bands of methane near 790 nm, and the $2\nu_1 + 2\nu_3$ band near 860 nm [1]. Scott et al. have investigated the possibility of methane detection with the use of a 1.34 μm Nd:YAG laser which can access the $\nu_1 + 2\nu_3$ combination-overtone band [2]. Uehara and Tai [3] have been used a diode laser to detect methane in air by monitoring absorption in the $2\nu_3$-stretch vibration-overtone band near 1.66 μm, achieving a detection limit of 0.3 ppm m with a signal averaging time of 1.3 s. This corresponds to 680 ppb m $(Hz)^{-1/2}$. Pavone and Inguscio [4] observed a component of the methane combination band corresponding to a third overtone at 866 nm.

The fundamental ν_3 band of methane near 3.2 μm, however, has transitions that are as much as a factor of 160 stronger than those of the first overtone band and may be better suited for sensitive detection. The maximum line intensity and the typical pressure broadening coefficient of methane in this band is 2.13×10^{-19} cm, and 0.027 MHz Pa^{-1}, respectively, which corresponds to a peak absorption of 0.005 m^{-1} ppm^{-1} in air at 1 atm near 3067 cm^{-1} [5]. Given the typical 1.8 ppm natural abundance of methane in air the absorption coefficient to be measured is 0.009 m^{-1}. The fundamental ν_3 band of methane is accessible by either conventional spectroscopy using the carbon monoxide overtone laser [6], the helium-neon laser near 3.39 μm [7], lead-salt diode lasers, color-center lasers, or with Ar^+-dye laser difference-frequency generation [8]. These infrared laser sources are also suitable for sensitive atmospheric trace gas detection. McManus et al. [9] demonstrated an atmospheric methane measurement instrument using a Zeeman-split helium-neon laser with a sensitivity of 20 ppb with a signal averaging time of 1 s (40 ppb $(Hz)^{-1/2}$). Simultaneous detection of methane and other gas species in air has been accomplished with the use of a compact lead-salt diode laser spectrometer that included a multipass absorption cell [10]. A detection limit for methane of 4 ppb m near 8 μm with a signal averaging time of 3 s was reported (14 ppb m $(Hz)^{-1/2}$).

However, each of the mid-infrared laser sources mentioned above suffers from its own specific practical drawbacks such as large physical size, lack of portability, high cost, high power consumption, poor tunability, or need for cryogenic cooling. On the other hand, the use of commercial single-frequency short wavelength diode lasers as pump sources offers benefits of small size, reliability, low cost, and low power consumption. These diode lasers also offer good amplitude and frequency stability which are important in the design of a compact and robust gas sensor. Several new interesting diode lasers operating in the 2.7 to 3.9 μm wavelength region have been developed [11–13] but are not yet commercially available. These lasers may still require cooling with liquid nitrogen for normal operation which is sometimes a

practical drawback. Therefore, CW Difference-Frequency Generation (DFG) pumped by visible and near-infrared diode lasers at room temperature remains an attractive technique for generation of tunable mid-infrared light [14].

In this paper, the applicability of CW diode-pumped DFG to the detection of methane in air is investigated. The detection limit is based upon the measured performance characteristics of the IR probe source and detector. A significant technical difficulty in applying DFG to spectroscopic detection is its low conversion efficiency when pumped directly by most single-frequency CW semiconductor lasers. Traveling-wave semiconductor amplifiers have been successfully applied to boost effective optical pump power [15]. In earlier work [16] we reported tunable CW mid-infrared DFG with output power in excess of 3 μW pumped by relatively low-power near-infrared diode lasers. A compact ring enhancement cavity was used in order to increase effective signal power available for difference-frequency mixing.

In this work, an improved and more robust design of the build-up cavity was implemented. Direct absorption and wavelength-modulation ($2f$) spectroscopy of methane in air at 10.7 kPa (80 torr) were performed in a 1 m single-pass cell with 1 μW probe power. The detection sensitivity of 12 ppb m $(Hz)^{-1/2}$ was limited by detector noise. In an effort to improve detection sensitivity, we tested the effectiveness of a confocal 3.2 μm enhancement cavity in combination with an intracavity absorption cell.

1 Diode-pumped cavity-enhanced 3.2 μm DFG source

A schematic diagram of the experimental setup is shown in Fig. 1. Two different compact lasers were used for pumping the difference-frequency IR source: a 500 mW diode-pumped monolithic Nd:YAG ring laser at 1064 nm (signal), and a 20 mW extended-cavity diode laser (ECDL) at 800 nm (pump). In later experiments, the ECDL was replaced with a 100 mW solitary laser diode in order to increase the IR power and allow fast wavelength modulation. The pump and signal laser beams were combined in a polarizing beamsplitter cube after spatial mode matching. They were then focused into a 5.5 mm antireflection-coated $AgGaS_2$ crystal through the input coupler of a bow-tie enhancement cavity. The cavity was designed to build up the 1064 nm light because bulk absorption in the crystal at that wavelength is lower than at 800 nm and scanning is simpler. The input coupler was a plano-concave fused silica substrate coated for high transmittance near 800 nm and 3.4% input coupling at 1064 nm. The radius of curvature of the concave side was 100 mm. The CaF_2 output coupler had the same dimensions and was coated for high reflection at 1064 nm. The transmittance of the output coupler was measured to be 41% near 3.2 μm using light from a carbon monoxide overtone laser. The long arm of the cavity was not a conventional bow-tie in that a Littrow prism reflector was used instead of a flat mirror. The function of this element was to eliminate multiple passes of the 800 nm light in the cavity. Use of a flat mirror resulted in a small portion of the diode laser

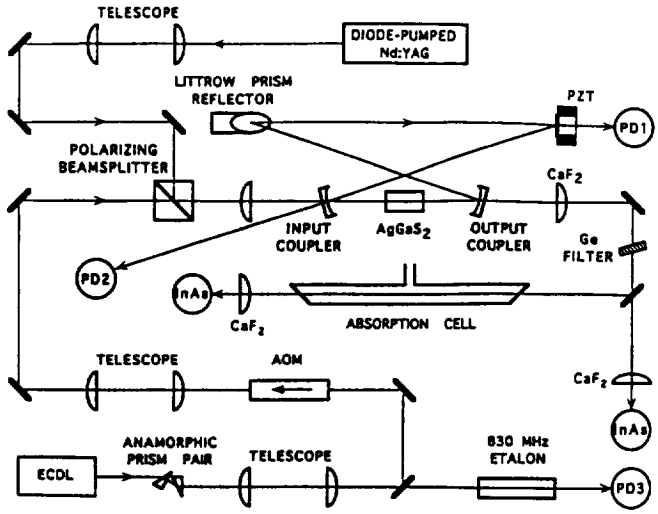

Fig. 1. Experimental setup for spectroscopic detection of methane near 3.2 μm in air. The $AgGaS_2$ crystal was placed into a bow-tie build-up cavity which was locked to resonance at 1064 nm. The 1064 nm light was supplied by a diode-pumped Nd:YAG laser. The tunable 800 nm light was supplied by either a grating tuned extended-cavity diode laser or a solitary laser diode. The IR power was stabilized by adjusting the diode laser power with an AOM

light circulating in the cavity which produced a systematic ripple in the IR power when the diode was tuned. The bow-tie cavity design with the addition of a Littrow prism reflector provides several advantages: it employs a minimum number of intracavity elements, is easy to align, has flexible mode diameter control, which is important for reaching optimum DFG conversion efficiency [17], and eliminates cavity resonance at the pump wavelength.

The Nd:YAG beam was spatially mode-matched to the cavity and the reflected power was monitored by a silicon photodetector PD2 (Fig. 1). Optimization of the cavity mode diameter allowed us to achieve a 90% input coupling efficiency limited mainly by the impedance mismatch of the input coupler transmittance. However, in normal operation a typical input coupling efficiency of between 75% and 85% was observed. The intracavity Nd:YAG power was monitored by a silicon photodetector PD1 which detected a 0.011% transmission through a PZT-driven flat cavity mirror (Fig. 1). The cavity build-up was 16 with the mixing crystal and 144 without. This corresponds to 6.1% and 0.7% excess cavity loss. Transmission losses in the crystal for the ordinary beam at 1064 nm have increased from 1.5% to 5.4% due to additional surface and bulk losses in the one-year time interval since the previous work [16]. Present measurements revealed 2.5% total reflection loss at 1064 nm compared to an immeasurably small reflection previously. This suggests that the index of refraction at the surface has changed. The manufacturer suggests that these changes are induced by exposure to near-UV light.

The 3.2 μm output beam (idler) was collimated by a CaF_2 lens, filtered by a broadband antireflection-coated germanium filter to remove pump and signal light, and focused by another CaF_2 lens onto a room-temperature InAs detector. A maximum of 6 μW IR power was measured with 40 mW pump power incident on the crystal, and

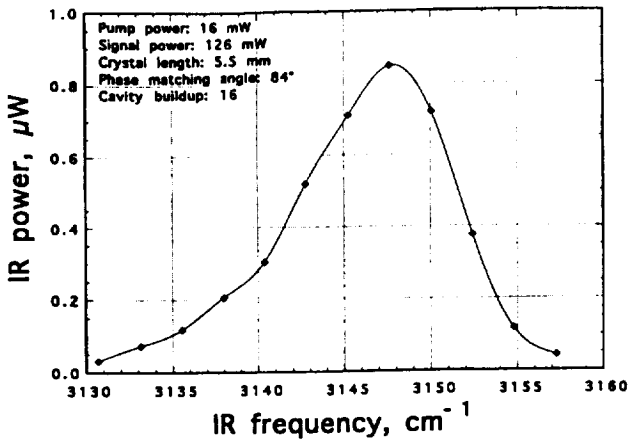

Fig. 2. Measured DFG power with pump wavelength near 800 nm for fixed phase matching angle. The full width at half maximum (FWHM) of the peak is 11 cm^{-1}. The asymmetry is a result of pumping with focused Gaussian beams

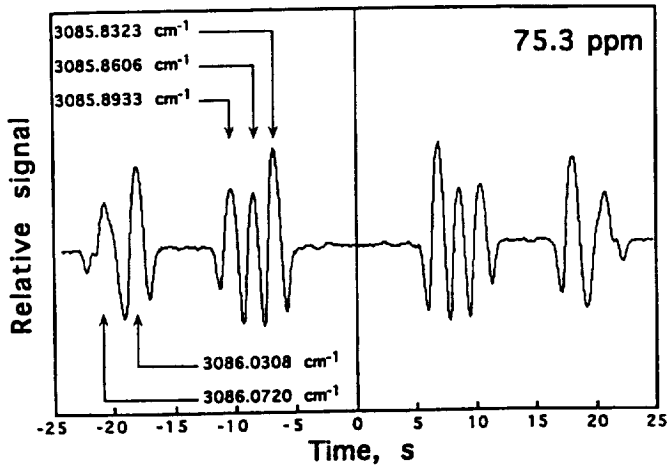

Fig. 3. Wavelength-modulation ($2f$) single-sweep spectrum of 75.3 ppm methane in 13.3 kPa (100 torr) air in a 59 cm cell. The spectrum was acquired by tuning of the solitary diode pump laser. Modulation frequency was 2 kHz, lock-in time constant was 0.1 s. The *vertical solid line at the center* indicates the point of sweep reversal

230 mW signal power in front of the cavity, which corresponds to 3.75 W intracavity signal power. Operation with more than 4.2 W intracavity Nd:YAG power was achieved, accompanied by noticeable thermal lensing in the mixing crystal. Frequency tuning of the idler wave was performed by tuning of the pump laser and crystal angle. At a fixed phasematching angle, frequency tuning over a range of approximately 10 cm^{-1} was possible as is apparent from Fig. 2. Therefore, short frequency scans of 10 GHz for spectroscopic measurements did not require crystal rotation. The observed asymmetry of the phasematching peak is a result of pumping with focused Gaussian beams [18]. Tuning of the pump laser from 801.3 nm to 795.2 nm and changing the internal phasematching angle of the crystal from 80° to 90° shifted the peak output IR power from 3076 to 3183 cm^{-1}. Operation at infrared frequencies below 3076 cm^{-1} was possible with phasematching angles below 80° but at the cost of more than 25% reduction in the output power due to larger beam walkoff, decreasing effective non-linear coefficient, and increasing Fresnel reflection losses at the AR-coated crystal surfaces which decreased the cavity build-up.

In the experiments described below the source was scanned by sweeping the frequency of the ECDL or solitary laser diode. In the ECDL, continuous mode-hop-free frequency tuning of 20 GHz was performed by electronically adjusted synchronous rotation and translation of the PZT-driven tuning mirror. The Littman configuration of the ECDL allowed tuning without steering of the output beam. The solitary laser diode was tuned by current and temperature control. Frequency scans of 10 GHz and wavelength modulation were performed by modulating the injection current. Fig. 3 shows a single-sweep $2f$ spectrum near 3086 cm^{-1} of 75.3 ppm methane in air at 13.3 kPa (100 torr) in a 59 cm single-pass cell. The spectrum was acquired by scanning the solitary diode pump laser. A low-finesse 830 MHz etalon was used for monitoring the scans.

The primary objective of the spectroscopic measurements was to determine a detection limit for methane in

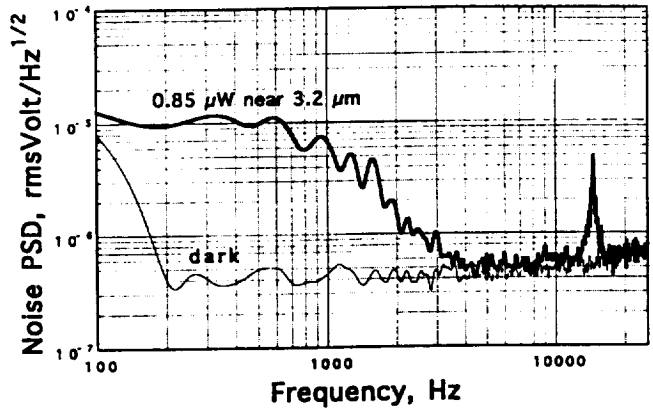

Fig. 4. The power spectral density of the noise from the InSb photodetector/preamplifier measured with a fast Fourier transform analyzer. The *upper curve* was taken when the detector was exposed to 0.85 μW of IR DFG radiation near 3.2 μm. Note that the buildup cavity locking noise dominates at frequencies below 3 kHz. The detector/preamplifier responsivity at 3.2 μm was 1.2×10^5 VW^{-1}

air using light produced by difference-frequency generation pumped by tunable diode lasers and to identify the sources of noise. Figure 4 shows plots of power spectral density of the amplitude noise in the IR detector signal acquired with a fast Fourier transform analyzer. In our $2f$ spectroscopic measurements, the maximum modulation frequency of the ECDL was limited to ~ 100 Hz resulting in demodulation frequencies below 200 Hz where the cavity locking noise still dominated.

In later experiments, a servo loop was used to reduce intensity noise in the IR beam. A portion of the IR beam was focused onto a room-temperature InAs reference detector, and the feedback adjustment of the diode laser power was performed by an acousto-optic modulator. This allowed the effects of the Nd:YAG build-up cavity noise, the amplitude modulation of the diode laser result-

ing from frequency tuning, and background fringes to be cancelled out.

In addition to single-pass absorption measurements we tested the effectiveness of a confocal enhancement cavity to improve the detection sensitivity. The cavity mirrors were plano-concave quartz substrates with 250 mm radius of curvature coated for high reflection at 3.4 μm. A transmittance of 1% was measured for each mirror using a probe beam from the DFG source. The finesse of the empty cavity was measured to be 213 which suggested a 0.5% additional loss in each mirror. For spectroscopic measurements an 18 cm long absorption cell with Brewster windows was placed into the cavity, reducing the cavity finesse to 182, which corresponds to an additional loss of about 0.25% per round trip. The cavity was dither-locked to resonance at the idler wavelength by controlling a PZT-driven mirror. In order to maintain the locking when the idler frequency was tuned, the diode laser sweep and modulation signals were supplied to the PZT controller that locked the 3.2 μm build-up cavity. Only 10% of the IR power from the DFG source could be coupled into the cavity because of poor spatial mode matching. Typical idler power delivered to the detector was only about 80 nW. With improved spatial mode matching of the IR beam, it should be possible to achieve 80% coupling into the cavity and deliver about 0.8 μW probe power to the detector.

2 Spectroscopic detection of methane in air

Direct absorption and wavelength-modulation ($2f$) spectroscopy of both pure methane and methane in air was performed with and without IR cavity enhancement. We used three calibrated mixtures of methane with natural air; these had mixing ratios of 75.3, 10.8 and 1.8 ppm. The last was natural air sampled on a mountain ridge.

Figure 5 shows experimental wavelength-modulation ($2f$) spectra of methane in natural air sample at 13.3 kPa (100 torr) in a 59 cm single-pass cell near 3086 cm^{-1}. This center frequency was chosen because of the presence of six strong distinct absorption lines of methane. For example, the transition at 3085.8323 cm^{-1} has a line intensity of 1.70×10^{-19} cm. It is only 20% weaker than the transition at 3067.3000 cm^{-1} which is the strongest in the band [5]. Tuning of the source to the frequency of this strongest line was possible at the cost of reduction in IR power output. For each of the spectra, the amplitude of the frequency modulation was optimized to produce the maximum $2f$ signal size. The spectra were taken without IR power stabilization.

Figure 6 shows direct absorption spectrum of the methane in natural air at 80 torr in a 1 m single-pass cell. It was acquired using a signal-averaging bandwidth of 1 Hz, and IR power stabilization. Atmospheric pressure-broadened methane in the laboratory air between the power stabilizer beamsplitter and the sample cell is visible in the baseline trace. The baseline slope is due to interference from a secondary reflection from the power stabilizer beamsplitter. Based upon the observed signal-to-noise ratio, a detection limit (signal-to-noise ratio of 1) of 12 ppb m $(Hz)^{-1/2}$ can be determined; it is in good agreement with the measured InAs detector noise. This corresponds to an absorbance root-mean-square noise of 5.1×10^{-5} $(Hz)^{-1/2}$. The detection limit can be improved. First, more IR probe power can be generated. For example, a commercial 1 W single-frequency master oscillator power amplifier (MOPA) can be used as a pump source at 800 nm. Also, a somewhat longer mixing crystal can be used. Second, better output coupler transmittance can be obtained. We have measured 60% transmittance at 3.2 μm for the replacement output coupler and 41% for that used in the experiment. Third, an IR detector with lower noise equivalent power (NEP) can be used. The room-temperature InAs detectors used in the experiment had NEPs of 17 pW $(Hz)^{-1/2}$ at 3.2 μm, which is a factor

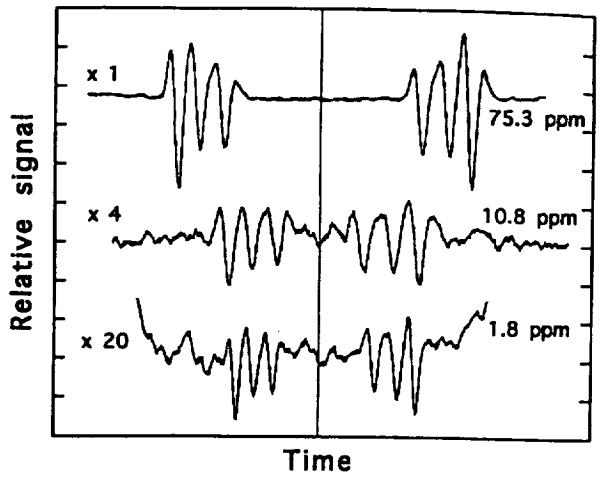

Fig. 5. Wavelength-modulation ($2f$) spectra of methane in air at 13.3 kPa (100 torr) in a 59 cm cell, obtained with 0.85 μW of IR probe power near 3086 cm^{-1}. Modulation frequency was 100 Hz. Sweep times were 50 s, 50 and 500 s, and lock-in amplifier time constants were 1 s, 1 s, and 3 s, respectively. The build-up cavity locking noise can be seen in the spectrum of 1.8 ppm methane. The scan widths were not the same for the 3 traces. The traces have been offset vertically for clarity

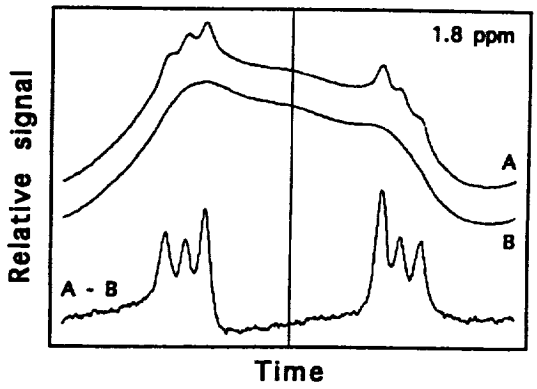

Fig. 6. Direct absorption spectrum of the methane in natural air near 3086 cm^{-1} at 10.7 kPa (80 torr) in a 1 m single-pass cell (A), and the evacuated cell (B). Atmospheric pressure-broadened methane in the laboratory air between the power stabilizer beamsplitter and the sample cell is visible in the baseline trace (B). The traces have been offset vertically for clarity. Both are 2000 sweep averages resulting in 1 Hz noise bandwidth for (A–B). The detection limit of 12 ppb m $(Hz)^{-1/2}$ can be inferred

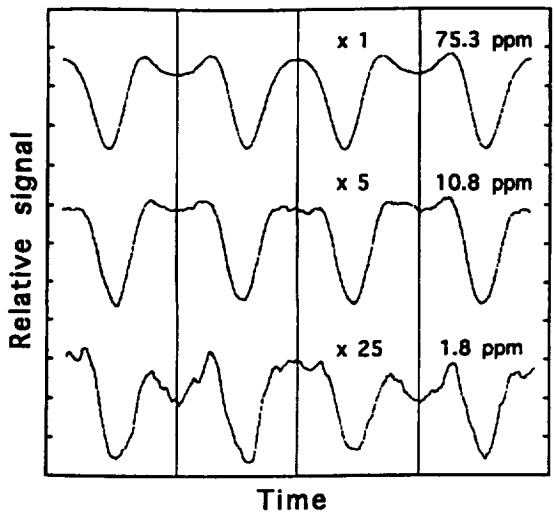

Fig. 7. Wavelength-modulation ($2f$) spectra of methane in air at 13.3 kPa (100 torr) in an 18 cm Brewster window cell inside a confocal enhancement cavity near 3.2 μm. The frequency of the transition is 3086.0308 cm^{-1}. The detected IR power was 80 nW, sweep time was 10 s, lock-in amplifier time constant was 0.3 s. A modulation frequency of 10 Hz was used to maintain locking of the IR cavity. The IR frequency sweep range was approximately 3 GHz in order to operate with reliable locking. The traces have been offset vertically for clarity. The *vertical solid lines* indicate points of sweep reversal

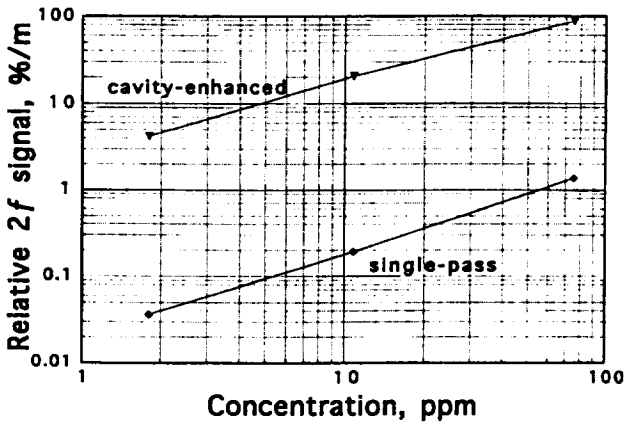

Fig. 8. Measured relative $2f$ signal amplitude per unit cell length $P_{2f}/(P_{0f}L)$ in the case of single-pass and cavity-enhanced detection, versus concentration of methane in air at 13.3 kPa (100 torr). The enhancement factor (max. 116) is in good agreement with the measured cavity finesse

of 5 larger than typical NEP of cooled InSb detectors. Fourth, either a multipass absorption cell or a build-up cavity can be used to increase effective path length.

The confocal enhancement cavity near 3.2 μm described above was used to increase the relative magnitude of the absorption signal. The effective number of passes in such cavity is

$$N = 2\frac{F}{\pi},$$

where F is the cavity finesse, and the factor 2 accounts for two passes through an intracavity absorption cell per round trip. Given the previously measured value of cavity finesse $F = 182$, the number of passes should be $N = 116$, which is in good agreement with the number obtained by comparing the fractional $2f$ signal per centimeter of cell length detected with cavity enhancement (Fig. 7) to that detected in the single-pass configuration (Fig. 5). The experimental enhancement factor for lower intracavity methane concentrations is in agreement with the experimental value of cavity finesse (Fig. 8). Higher concentrations of methane introduce more absorption per round trip thus decreasing the cavity finesse and the related effective number of passes which is the case with the 75.3 ppm sample.

3 Conclusion

In summary, spectroscopic detection of the methane in natural air (1.8 ppmv) using diode-laser pumped cavity-enhanced CW tunable difference-frequency generation near 3.2 μm has been performed by four methods: direct absorption spectroscopy, second-harmonic detection wavelength modulation spectroscopy, cavity-enhanced second-harmonic detection wavelength modulation spectroscopy, and direct absorption spectroscopy with power stabilization. The spectroscopic DFG source was pumped with an 800 nm diode laser and a diode-pumped 1064 nm Nd:YAG laser. It delivered a maximum of 6 μW of narrowband infrared light with 40 mW pump power and 230 mW signal power and was tunable from 3076 to 3183 cm^{-1}.

With no cryogenic components, we observed a noise equivalent concentration for the detection of methane in air at 80 torr of 12 ppb $(Hz)^{-1/2}$ using a 1 m cell and direct absorption spectroscopy with power stabilization. This corresponds to an absorbance root-mean-square noise of 5.1×10^{-5} $(Hz)^{-1/2}$. We have observed the methane in natural air at atmospheric pressure, as can be seen from the baseline trace in Fig. 6. The competing effects of increased methane density and pressure broadening compared to 80 torr cancel out so the expected detection limit would be the same.

By using an output coupler with higher transmittance, and using thermoelectrically cooled HgCdTe detectors with 5 times better noise equivalent power, we expect to be able to observe a noise equivalent column density of 1.6 ppb m $(Hz)^{-1/2}$. Proper spatial mode matching into the 3.2 μm build-up cavity would yield an effective path length of 15 m and thus a predicted detection limit of 0.1 ppb $(Hz)^{-1/2}$. Alternatively, a White cell could also be used. The choice of build-up cavity or multipass cell would be dictated by application-dependent constraints such as physical size and sample volume. With either the build-up cavity or a multipass cell stray interference fringes or other baseline effects may limit the actual performance before the predicted 0.1 ppb $(Hz)^{-1/2}$ detection limit is reached.

Acknowledgements. The authors are grateful to Joe Wells for helping with measurements requiring the use of the carbon monoxide laser and Tamara Zibrova for the special coatings. The work was supported in part by the National Science Foundation, and the Robert A. Welch Foundation.

References

1. A. Lucchesini, I. Longo, C. Gabbanini, S. Gozzini, L. Moi: Appl. Opt. **32**, 5211 (1993)
2. J.C. Scott, R.A. Maddever, A.T. Paton: Appl. Opt. **31**, 815 (1992)
3. K. Uehara, H. Tai: Appl. Opt. **31**, 809 (1992)
4. F.S. Pavone, M. Inguscio: Appl. Phys. B **56**, 118 (1993)
5. GEISA database, Laboratoire de Meteorologie Dynamique DU C.N.R.S., Ecole Polytechnique, F-91128 Palaiseau Cedex, France
6. E. Bachem, A. Dax, T. Fink, A. Weidenfeller, M. Schneider, W. Urban: Appl. Phys. B **57**, 185 (1993)
7. C.B. Moore: Appl. Opt. **4**, 252 (1965)
8. A.S. Pine: J. Opt. Soc. Am. **66**, 97 (1976)
9. J.B. McManus, C.E. Kolb, P.L. Kebabian: Appl. Opt. **28**, 5016 (1989)
10. C.R. Webster, R.D. May, C. A. Trimble, R. G. Chave, J. Kendall: Appl. Opt. **33**, 454 (1994)
11. H.K. Choi, G.W. Turner, Z.L. Liau: Appl. Phys. Lett. **65**, 2251 (1994)
12. A.N. Baranov, A.N. Imenkov, V.V. Sherstnev, Yu. P. Yakovlev: Appl. Phys. Lett. **64**, 2480 (1994)
13. J. Faist, F. Capasso, D.L. Sivco, C. Sirtori, A.L. Hutchinson, A.Y. Cho: Science **246**, 553 (April 1994)
14. U. Simon, C.E. Miller, C.C. Bradley, R.G. Hulet, R.F. Curl, F.K. Tittel: Opt. Lett. **18**, 1062 (1993)
15. U. Simon, F.K. Tittel, L. Goldberg: Opt. Lett. **18**, 1931 (1993)
16. U. Simon, S. Waltman, I. Loa, L. Hollberg, F. Tittel: J. Opt. Soc. Am. B **12**, 323 (1995)
17. Tran-Ba-Chu, M. Broyer: J. Phys. (Paris) **46**, 523 (1985)
18. G.D. Boyd, D.A. Kleinman: J. Appl. Phys. **39**, 3597 (1968)

Detection of CO in air by diode-pumped 4.6-μm difference-frequency generation in quasi-phase-matched $LiNbO_3$

K. P. Petrov

Department of Electrical and Computer Engineering, Rice University, Houston, Texas 77251-1892

L. Goldberg and W. K. Burns

Naval Research Laboratory, Washington, D.C. 20375-5672

R. F. Curl

Department of Chemistry, Rice University, Houston, Texas 77251-1892

F. K. Tittel

Department of Electrical and Computer Engineering, Rice University, Houston, Texas 77251-1892

Received August 10, 1995

Detection of CO, N_2O, and CO_2 in ambient air was performed with a room-temperature cw IR source based on difference-frequency generation in periodically poled $LiNbO_3$. The source was pumped by a seeded high-power GaAlAs amplifier at 860 nm and a diode-pumped monolithic Nd:YAG ring laser at 1064 nm. The IR output was tunable between 2160 and 2320 cm^{-1} without crystal rotation. The CO detection sensitivity is extrapolated to 5 ppb m/$\sqrt{Hz}$ if limited by IR intensity noise. © 1996 Optical Society of America

The use of quasi-phase-matched periodically poled lithium niobate (PPLN) for mid-IR difference-frequency generation (DFG) and optical parametric oscillators was reported recently.[1–4] This new material offers the advantages of a large effective nonlinear coefficient and a phase-matching condition that can be designed for pumping with various visible and near-IR lasers. Here we report the use of a PPLN crystal tailored to match the generally available high-power diode and diode-pumped lasers at 860 and 1064 nm.[1] At these pump wavelengths the phase-matching condition is nearly independent of the idler wavelength, permitting tuning of the DFG between 4.0 and 4.5 μm without crystal rotation.[4] This wavelength region contains strong fundamental absorption bands of several important air pollutants[5] such as carbon monoxide (CO), nitrous oxide (N_2O), carbon dioxide (CO_2), and sulfur dioxide (SO_2) and is currently not conveniently accessible by room-temperature cw single-frequency diode lasers.

We have investigated the feasibility of application of a PPLN-based diode-pumped DFG source to spectroscopic trace gas detection in air. The performance characteristics of the source, including output power, linewidth, tuning range, and amplitude noise, were examined from the standpoint of spectroscopic detection. Atmospheric CO, N_2O, and CO_2 were used as sample target species. A detection limit for CO of 5 parts in 10^9 (ppb) m/$\sqrt{Hz}$ was found for wavelength-modulation $2f$ spectroscopy in ambient air under interference-free conditions.

The tunable mid-IR DFG source, shown in Fig. 1, mixed a Nd:YAG and a high-power tapered GaAlAs semiconductor amplifier pump. Although the source is similar to the source described in Ref. 4, it differs from it in two important ways: (i) for compactness and narrow linewidth the previously used lamp-pumped Nd:YAG is replaced with a diode-pumped monolithic nonplanar ring laser emitting 237 mW of power in a single longitudinal mode and (ii) the previously used external grating cavity tunable laser based on a tapered amplifier is replaced with a tapered amplifier seeded by a single-frequency laser diode, permitting fast frequency tuning by means of current modulation. The seed laser (SDL, Inc., Model 5410) was isolated from the tapered amplifier by a 40-dB Faraday isolator and was temperature stabilized to $\pm 0.02\,^{\circ}C$, yielding a frequency stability of ± 0.6 GHz. To eliminate feedback-induced spectral instabilities, a low-numerical-aperture lens was used for seed laser collimation at a working distance of ~ 1 cm. A low lens collection efficiency resulted in 12-mW seed power incident upon the tapered amplifier (SDL, Inc., Model 8630), which near its 860-nm gain peak emitted 1.25 W at a current of 2.0 A. The amplifier emission was collimated by a spherical ($f = 4.5$ mm) and a cylindrical ($f = 15$ cm) lens[4] and passed through a Faraday isolator, a dichroic beam splitter, and an $f = 5$ cm focusing lens, producing 820 mW of power at the input facet of a 6-mm-long PPLN crystal. The field-poled, z-cut crystal had a domain period of 22.6 μm and was oriented $\sim 10^{\circ}$ relative to the beam to yield wideband phase matching in the 4.3–4.6-μm range.[4] With 220 mW of incident power at 1064 nm, a maximum of 8.0 μW was measured at 4.5 μm. A somewhat lower conversion

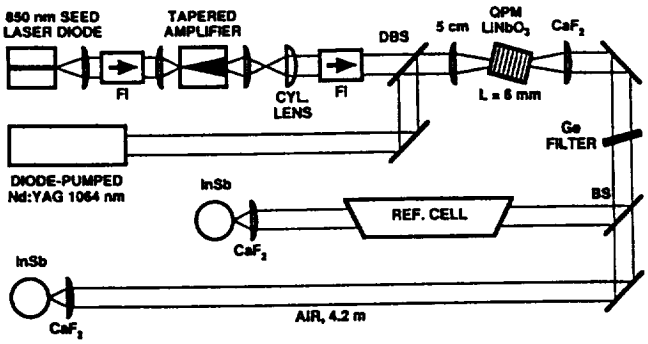

Fig. 1. Schematic of the tunable cw mid-IR DFG source used for detection of CO, N_2O, and CO_2 in air. The nonlinear mixing element was a quasi-phase-matched (QPM) periodically poled $LiNbO_3$ crystal. FI's, Faraday isolators; DBS, dichroic beam splitter; BS, beam splitter.

efficiency[1,4] observed here is attributed to nonoptimized beam diameters. The amplifier was typically operated to produce DFG power of ~3.0 μW, adequate for all the measurements described below.

The spectrum of the seeded amplifier was monitored with an optical spectrum analyzer and a Fabry–Perot interferometer. The linewidth was less than the 50-MHz resolution of the interferometer. Coarse and fine wavelength adjustments were carried out with seed laser temperature and bias current settings, respectively. We made frequency scans by superimposing a 30-mA peak-to-peak triangular waveform at ~10 Hz on the seed laser bias current, resulting in a continuous mode-hop-free frequency sweep range of 80 GHz. An additional $f = 2$ kHz sinusoidal waveform was used for frequency modulation during scans, with up to 11 GHz peak-to-peak frequency modulation amplitude.

Frequency sweep and modulation were accompanied by linear modulation of the seed power. This modulation was greatly suppressed by the clamped input-versus-output power transfer function of the tapered amplifier operated in a regime close to saturation. Because of the relatively low seed power, however, the saturation was incomplete, and the nonlinearity of the amplifier power transfer function produced the second harmonic of the modulation frequency, causing a weak rolling baseline in the $2f$ IR spectra. This effect can be reduced by increasing the seed power.

Another undesirable effect observed initially was weak étalon interference between the two facets of the tapered amplifier. This interference resulted in the DFG power modulation during scan, which masked the gas absorption signal. During the 80-GHz scan the seed wavelength tuned across four amplifier étalon fringes spaced by approximately 20 GHz. To eliminate this effect we synchronously modulated the amplifier current with the ramp used for seed laser frequency scans. This caused, through temperature- and carrier-density-induced index variation, a proportional scan of étalon fringe wavelength. With proper adjustment of the ramp amplitude (~200 mA) and phase the étalon fringe wavelength excursion matched that of the seed laser, and the power modulation caused by interference was eliminated. Improved antireflection coating of the diode amplifier chip could reduce étalon effects, making the injection current modulation unnecessary.

The intensity noise spectrum of the DFG source was measured with a spectrum analyzer, and the results are shown in Fig. 2. The relative intensity noise was $3 \times 10^{-5}/\sqrt{\text{Hz}}$ at frequencies above 1 kHz. We expect a reduction in the intensity noise with the use of a low-noise amplifier current supply.

The observed continuous tuning range of the source was 2160–2320 cm^{-1}, which was sufficient for detection of CO, N_2O, and CO_2 in air. Typical abundances of these species in natural air are 330 parts in 10^6 (ppm), 320 ppb, and 150 ppb, respectively.[7] Figure 3 shows direct-absorption and wavelength-modulation $1f$ and $2f$ spectra of CO_2 in 2.5-m ambient air near 2303 cm^{-1}. We have not compared noise in the $1f$ and $2f$ signals. If the $1f$ signal from a reference sample is used to lock the IR frequency to the center of a given molecular transition, the $2f$ signal conveniently measures peak absorption. The traces are symmetric with respect to the vertical line at the center, which indicates reversal of the 2.5-cm^{-1} frequency sweep. Atmospheric CO_2 is the dominant absorber in this wavelength region because of its relatively high natural abundance. Absorption by the less

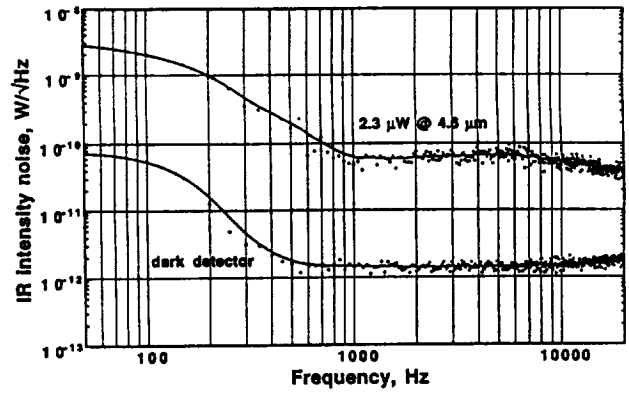

Fig. 2. Rms intensity noise in the IR beam. The data were acquired with a rf spectrum analyzer and converted to units of $W/\sqrt{\text{Hz}}$.

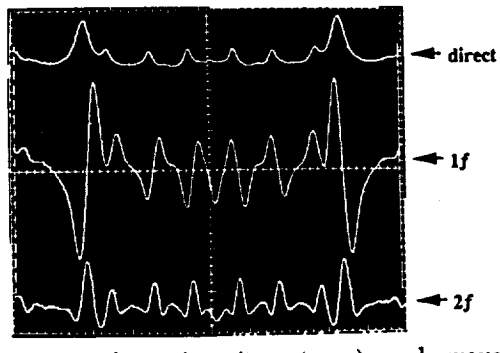

Fig. 3. Direct-absorption (top trace) and wavelength-modulation $1f$ and $2f$ (middle and bottom traces, shown on the same vertical scale) spectra of CO_2 in 2.5-m ambient air near 2303 cm^{-1} recorded with a digital scope. The frequency sweep of 2.5 cm^{-1} is reversed at the center. The transitions seen here are $P(50)$ (0001–0000), $R(26)$ (0001–0000), $P(39)$ (0111–0110), and $R(24)$ (0001–0000), from left to right in the left half of the figure.[5] Both R transitions belong to $^{16}O^{13}C^{16}O$.

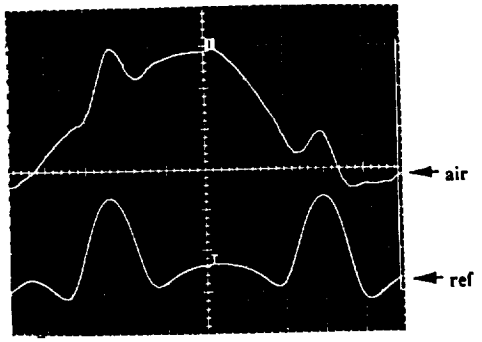

Fig. 4. Wavelength-modulation $2f$ spectra of the $R(6)$ fundamental of CO at 2169 cm^{-1} in 4.2-m ambient air (30× magnified, top), and a reference sample (~3-Torr CO mixed with room air in a 10-cm cell, bottom). The frequency sweep of ~20 GHz is reversed at the center. The sweep rate was 10.6 Hz, the modulation frequency was 2 kHz, and the lock-in time constant was 1 ms. Both traces are 100-sweep averages.

abundant N_2O and CO, even at the peak (1.1×10^{-2} and 6.0×10^{-3} ppm^{-1} m^{-1}, respectively), can be completely swamped by H_2O absorption.

The ambient CO and N_2O were monitored over the 4.2-m open path between the mixing crystal and the signal detector. Figure 4 shows wavelength-modulation $2f$ spectra of the $R(6)$ fundamental of CO near 2169 cm^{-1} in air and in a reference sample. The sample had ~3 Torr of CO mixed with air at atmospheric pressure in a 10-cm cell, resulting in 93% peak absorption. The $2f$ absorption signal was monitored to permit easy visual comparison of position and width of the signal and reference absorption peaks. The vertical line at the center indicates reversal of the frequency sweep, which was approximately 20 GHz. Both traces are 100-sweep averages, resulting in the noise bandwidth of 2.5 Hz. The rolling baseline in the air trace is a result of synchronous amplitude modulation in the tapered amplifier, as mentioned above. It is asymmetric because of weak thermal modulation in the amplifier caused by the frequency sweep and delayed in time. Magnitudes of absorption peaks in the top trace suggest that the concentration of CO in laboratory air is ~360 ppb, which is higher than the U.S. standard average 150 ppb.[7] The rms noise in the $2f$ absorption signal measured without frequency sweep was approximately equal to the rms intensity noise (see Fig. 2). This corresponds to a noise equivalent column density of 5 ppb m/$\sqrt{\text{Hz}}$ for CO in air at atmospheric pressure. This is comparable to the detection limit of 14 ppb m/$\sqrt{\text{Hz}}$ for CH_4 in air near 8 μm (peak absorption of 1.8×10^{-3} ppm^{-1} m^{-1} at 1306 cm^{-1}) in a compact lead-salt diode laser spectrometer[8] reported by Webster *et al.*

Potentially the tuning range can be extended to 4.0 μm to permit the detection of SO_2. In our experiment, tuning to wavelengths below 4.3 μm required cooling of the seed laser below 15 °C, and to avoid water condensation we did not perform it. The use of an external cavity laser can provide the desired tuning range without extreme heating or cooling.[4] Alternatively, seed lasers with lower operating wavelengths could be used. DFG wavelengths from 3.0 to 5.5 μm have been generated with PPLN.[4] A wavelength of particular interest is the 5.3-μm fundamental R branch of nitric oxide. At this wavelength we measured a transmission of 75% in a 1-mm-long uncoated $LiNbO_3$ sample. For a 6-mm-long uncoated sample this implies a 42% transmission. For access to the wavelength of 5.3 μm, a seed laser emitting at 886 nm would be required in the present DFG source, or the Nd:YAG could be replaced by a 1025-nm laser diode.

In summary, water-free detection of the CO in ambient air (360 ppb) was performed with a compact tunable laser source at 4.6 μm. The source was based on DFG in quasi-phase-matched $LiNbO_3$ pumped by a seeded high-power GaAlAs amplifier at 860 nm and a diode-pumped Nd:YAG laser at 1064 nm. The CO detection sensitivity of 5 ppb m/$\sqrt{\text{Hz}}$ is extrapolated based on rms noise measured in the $2f$ infrared spectra. This constitutes an important demonstration of sensitive detection of CO rovibrational fundamental in air by a room-temperature diode-pumped tunable cw laser source. Tuning of the DFG source between 2160 and 2320 cm^{-1} was observed, limited by the tuning range of the solitary diode seed laser. This was sufficient for detection of CO, N_2O, and CO_2 and in the future can be extended to 2500 cm^{-1} for detection of SO_2 and to 1900 cm^{-1} for the detection of nitric oxide.

This research was supported in part by the National Science Foundation, the National Aeronautics and Space Administration, the Robert A. Welch Foundation, and the U.S. Office of Naval Research.

References

1. L. Goldberg, W. K. Burns, and R. W. McElhanon, Opt. Lett. **20,** 1280 (1995).
2. S. Sanders, R. J. Lang, L. E. Myers, M. M. Fejer, and R. L. Byer, in *Conference on Lasers and Electro-Optics,* Vol. 15 of 1995 OSA Technical Digest Series (Optical Society of America, Washington, D.C., 1995), p. 370.
3. L. E. Myers, G. D. Miller, R. C. Eckardt, M. M. Fejer, and R. L. Byer, Opt. Lett. **20,** 52 (1995).
4. L. Goldberg, W. K. Burns, and R. W. McElhanon, Appl. Phys. Lett. **67,** 2910 (1995).
5. GEISA database (LMD Centre National de l'Ecole Polytechnique, 91128, Palaiseau Cedex, France).
6. U. Simon, F. K. Tittel, and L. Goldberg, Opt. Lett. **18,** 1931 (1993).
7. D. K. Killinger, J. H. Churnside, and L. S. Rothman, in *Fundamentals, Techniques, and Design,* Vol. 1 of Handbook of Optics, 2nd ed., M. Bass, E. W. Van Stryland, D. R. Williams, and W. L. Wolfe, eds. (McGraw-Hill, New York, 1995), Chap. 44, p. 5.
8. C. R. Webster, R. D. May, C. A. Trimble, R. G. Chave, and J. Kendall, Appl. Opt. **33,** 454 (1994).

Continuous-wave tunable 8.7-μm spectroscopic source pumped by fiber-coupled communications lasers

K. P. Petrov, R. F. Curl, and F. K. Tittel

Rice Quantum Institute, Rice University, Houston, Texas 77251-1892

L. Goldberg

Optical Sciences Division, Naval Research Laboratory, Washington, D.C. 20375-5672

Received May 7, 1996

Tunable narrow-band cw difference-frequency generation at 8.7 μm was demonstrated in silver gallium selenide ($AgGaSe_2$) at room temperature. The crystal was pumped by an injection-seeded Er/Yb-codoped fiber amplifier at 1.554 μm and a fiber-coupled diode-pumped monolithic ring Nd:YAG laser at 1.319 μm. The difference-frequency output was used for high-resolution spectroscopy of sulfur dioxide (SO_2). © 1996 Optical Society of America

The 8–12-μm wavelength region has been a target of high-resolution molecular spectroscopy and trace gas detection for many years, but the choice of a tunable cw narrow-band source operating in this region has been limited to lead-salt diode lasers and carbon dioxide lasers. These sources, although they are suitable for high-resolution molecular spectroscopy, suffer practical drawbacks such as large size, high power consumption and lack of wavelength tunability, and the need for cryogenic cooling. The use of diode lasers operating at the wavelengths of 1.3 and 1.5 μm as pump sources for difference-frequency generation (DFG) in $AgGaSe_2$ was proposed by Simon *et al.* in 1993.[1] The advantage of this scheme is the possibility of convenient generation of cw tunable narrow-band light in the spectroscopic fingerprint region 8–12 μm by readily available communications diode lasers. In addition, the use of fiber coupling for these sources can be expected to improve stability, eliminate the need for optical alignment, reduce the size, and lower the cost of the DFG source.

The recent development of Er/Yb-codoped fiber amplifiers[2] near 1.5 μm and of Pr^{3+}-doped fluoride fiber amplifiers[3] near 1.3 μm has made optical single-frequency output power in excess of 100 mW available. Such sources can be used for tunable low-noise cw DFG at the microwatt level between 8 and 12 μm. This radiation can be used for high-resolution mid-infrared molecular spectroscopy and, potentially, for spectroscopic detection and measurement of trace air contaminants such as ammonia, ethylene, sulfur dioxide, methane, nitrous oxide, and phosphine.

Here we report the implementation and successful operation of a compact all-solid-state room-temperature DFG source (see Fig. 1) that employed a high-power Er/Yb-codoped fiber amplifier pumped at 1.064 μm. The amplifier was injection seeded by an optically isolated 2-mW pigtailed distributed-feedback (DFB) diode laser at 1.554 μm and operated near saturation, producing as much as 0.5 W of single-frequency power. Figure 2 shows the amplifier output power with injection seeding versus launched pump power at 1.064 μm. The pump threshold of 87 mW and a slope efficiency of 12% were determined from these data. The relatively low[2] slope efficiency is attributed to incomplete saturation, a nonoptimal copropagating pump arrangement, and operation at a wavelength that is ~20 nm away from the gain peak. After optical isolation, which was accompanied by a 20% loss in power, the amplifier output was combined with the output of a 35-mW diode-pumped monolithic ring Nd:YAG laser (Lightwave Electronics Model 122) at 1.319 μm in a polarizing cube beam splitter.

Later in the experiment an alternative optical setup was implemented in which the pump (1.319 μm) and the signal (1.554 μm) beams were combined in a single-mode fiber by a fiber-optic wavelength-division multiplexer. This arrangement provided the stable, alignment-free spatial and angular beam overlap required for optimal DFG conversion efficiency. In both cases the polarization controllers were adjusted to produce linear orthogonal polarizations of the pump and the signal beams at the crystal input.

The difference-frequency mixing was performed in a 4 mm × 4 mm × 10 mm $AgGaSe_2$ crystal (Cleveland

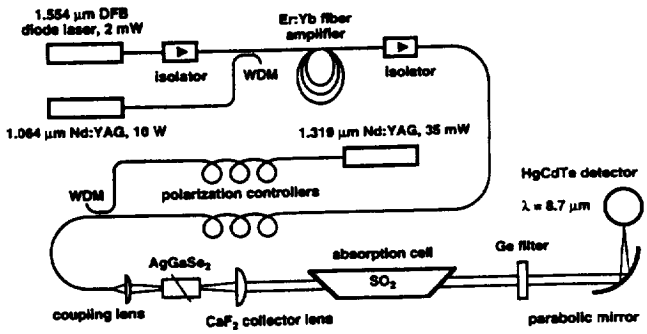

Fig. 1. Schematic of an 8.7-μm tunable single-frequency cw DFG source pumped by fiber-coupled diode and solid-state lasers operating at 1.319 and 1.554 μm. A wavelength-division multiplexer (WDM) was used to combine the two beams in a single fiber before mixing so that no adjustment of the beam overlap was necessary. The source was used for high-resolution spectroscopy of SO_2.

0146-9592/96/181451-03$10.00/0

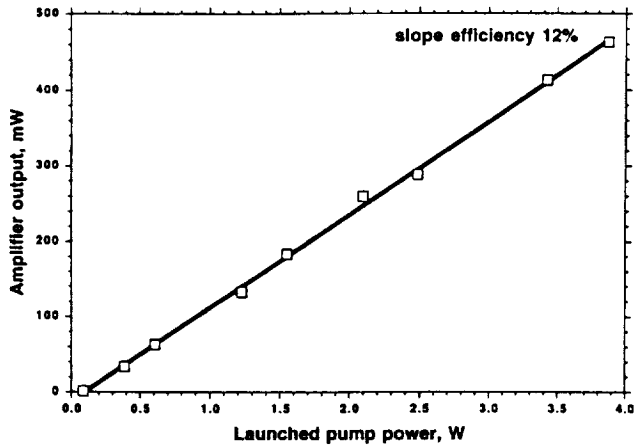

Fig. 2. Output power from an Er/Yb-codoped fiber amplifier before a Faraday isolator versus launched pump power at 1.064 μm. The amplifier is injection seeded by a 2-mW DFB diode laser at 1.554 μm.

Crystals, Inc.) cut for type 1 phase matching at an internal angle of 65°. The actual phase-matching angle θ used in the experiment was 68.4°, which was readily accessible with a given crystal aperture and required an external incidence angle of 9°. In the arrangement using the polarizing cube beam splitter the pump and the signal beams were focused into the mixing crystal by an $f = 5$ cm lens. The beam waists inside the crystal were 15.5 and 18.8 μm, respectively, calculated from the measured waists of collimated beams. No attempt was made to achieve optimal focusing.[4] The effective crystal length was limited by the birefringent beam walk-off:

$$\tan \rho = 1/2 \sin 2\theta n(\lambda, \theta)^2 |n_e(\lambda)^{-2} - n_0(\lambda)^{-2}|.$$

Here $n_0(\lambda)$, $n_e(\lambda)$, and $n(\lambda, \theta)$ are the ordinary, the extraordinary, and the angle-dependent indices of refraction respectively, of $AgGaSe_2$.[5] The walk-off angle calculated for the pump wavelength of 1.319 μm is 0.39°, which corresponds to an effective crystal length of 2.5 mm.

The difference-frequency output at 8.7 μm (idler) was collected by an $f = 5$ cm CaF_2 lens, transmitted through a 4-mm-thick uncoated Ge filter, and focused onto a liquid-N_2-cooled HgCdTe detector by an $f = 5$ cm off-axis parabolic mirror. With 29-mW pump power and 370-mW signal power incident upon the crystal, an idler power of 0.1 μW was measured. After correction for reflection losses from the uncoated Ge filter and facets of the $AgGaSe_2$ crystal, this corresponds to 0.4 μW of power generated inside the crystal. This power level is 35% less than expected from a 2.5-mm-long crystal under the conditions of optimal focusing.[4] This discrepancy may be attributed in part to improper mode matching of the pump and the signal beams. However, it was also established in the course of the experiment that the detector active area of 0.25 mm^2 was not sufficient to collect all the idler output because of the larger spot size at the focus of the parabolic mirror. The spot size was increased primarily by improper alignment of the mirror and by spherical aberrations in the collector lens that was used to collimate a rapidly diverging idler beam 8.7 μm.

The typical detected idler power 0.1 μW was sufficient for high-resolution spectroscopy considering that the noise equivalent power the HgCdTe detector was 3×10^{-12} W/$\sqrt{\text{Hz}}$, which corresponds to an equivalent absorption of $3 \times 10^{-5}/\sqrt{\text{Hz}}$. A 10-cm-long absorption cell with CaF_2 Brewster windows filled to 5 Torr with sulfur dioxide was introduced into the idler beam for spectroscopic measurements. Initially, we performed the frequency tuning by sweeping the drive current of the DFB seed laser at 1.554 μm. However, the current tuning response of the laser was not sufficient to permit frequency scans longer than 5 GHz, thereby making it difficult to identify the observed absorption lines. We therefore used instead temperature tuning of the Nd:YAG pump laser at 1.319 μm. A tuning rate of 0.02 Hz was selected to permit faster data acquisition without distortion of linearity of the frequency sweep. The pump beam was chopped at a rate of 2 kHz. The idler power was lock-in detected without regard to phase and recorded with an 8-bit digital oscilloscope. The observed infrared transitions of sulfur dioxide were assigned by a HITRAN database.[6] Figure 3 shows the direct absorption spectrum of the ν_1 symmetric stretch band of sulfur dioxide near 1144 cm^{-1}. The frequency sweep was reproducible and linear over at least half of a wave number, which is the maximum continuous sweep range available with the pump laser used in this experiment.

In summary, we have demonstrated an all-solid-state room-temperature cw narrow-band source tunable near 8.7 μm. The source is based on difference-frequency mixing of a fiber-coupled diode-pumped monolithic ring Nd:YAG laser 1.319 μm and an Er/Yb-copdoped fiber amplifier in type 1 critically phase-matched $AgGaSe_2$. The fiber amplifier was pumped at 1.064 μm and injection seeded by a pigtailed DFB laser diode at 1.554 μm. Alternatively, a 1.3-μm extended-cavity diode laser in conjunction with a Pr^{3+}-doped fluoride fiber amplifier can replace the Nd:YAG laser at 1.319 μm, thereby providing higher

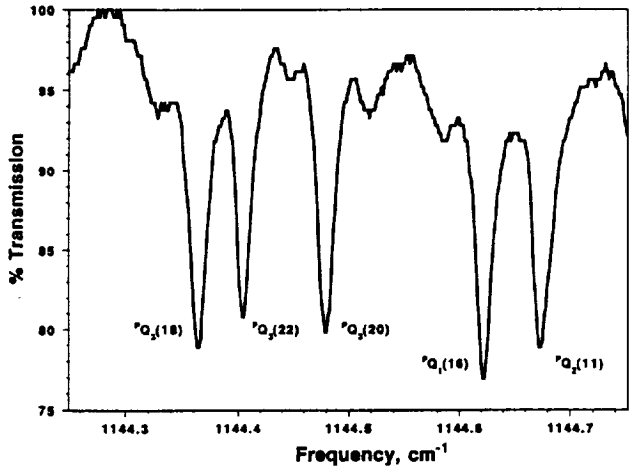

Fig. 3. Optical transmission of 10-cm-long Brewster window absorption cell filled with SO_2 at a pressure of 5 Torr. The sweep time was 50 s, the lock-in amplifier time constant was 0.1 s (12 dB/octave roll-off), and the choppler frequency was 2 kHz. The signal was detected without regard to phase (R component).

pump power and permitting fast continuous frequency scans of 10 cm^{-1} or more. With 29 mW of pump power and 370 mW of signal power incident upon the mixing crystal, 0.1-μW idler power was detected. The DFG source was applied to high-resolution spectroscopy of the ν_1 symmetric stretch band of SO_2. This, to our knowledge, is the first reported cw all-diode-pumped spectroscopic DFG source operating at a wavelength above 8 μm at room temperature. Furthermore, the source uses commercial single-frequency pigtailed diode and diode-pumped solid-state lasers operating near the fiber communications wavelengths of 1.3 and 1.5 μm. Although limited infrared tuning range and output power have been demonstrated in the experiment, both can be improved by replacement of the pump sources. With the use of two 300-mW fiber amplifiers injection seeded by tunable extended-cavity diode lasers near 1.3 and 1.5 μm, for example, the DFG output power can be increased to 5 μW, whereas the tuning range can be extended from 900 to 1400 cm^{-1}. These projected performance characteristics will benefit applications such as high-resolution molecular spectroscopy and trace-gas detection.

The authors are grateful to L. W. Hollberg and S. Waltman for providing the $AgGaSe_2$ crystal. The research was supported in part by the National Aeronautics and Space Administration, the National Science Foundation, the Texas Advanced Technology Program, The Welch Foundation and the U.S. Office of Naval Research.

References

1. U. Simon, Z. Benko, M. W. Sigrist, R. F. Curl, and F. K. Tittel, Appl. Opt. **32,** 6650 (1993).
2. S. G. Grubb, W. F. Humer, R. S. Cannon, T. H. Windhorn, S. W. Vendetta, K. L. Sweeney, P. A. Leilabady, W. L. Barnes, K. P. Jedrzejewski, and J. E. Townsend, IEEE Photon. Technol. Lett. **4,** 553 (1992).
3. T. J. Whitley, J. Lightwave Technol. **13,** 744 (1995).
4. Tran-Ba-Chu and M. Broyer, J. Phys. (Paris) **46,** 523 (1985).
5. D. Roberts, Appl. Opt. **35,** 4677 (1996).
6. L. S. Rothman, R. R. Gamache, A. Goldman, L. R. Brown, R. A. Toth, H. M. Pickett, R. L. Poynter, J.-M. Flaud, C. Camy-Peyret, A. Barbe, N. Husson, C. P. Rinsland, and M. A. H. Smith, Appl. Opt. **26,** 4058 (1987).

Appl. Phys. B 63, 437–441 (1996)

Applied Physics B Lasers and Optics

A continuously tunable long-wavelength cw IR source for high-resolution spectroscopy and trace-gas detection

Wade C. Eckhoff[1], Roger S. Putnam[3], Shunxi Wang[2], Robert F. Curl[1], Frank K. Tittel[2]

[1] Department of Chemistry and Rice Quantum Institute, William Marsh Rice University, 6100 Main St., Houston, TX 77251-1892, USA
[2] Department of Electrical and Computer Engineering and Rice Quantum Institute, William Marsh Rice University, 6100 Main St., Houston, TX 77251-1892, USA
[3] Aerodyne Research Inc., 45 Manning Road, Billerica, MA 01821-3976, USA

Received: 1 April 1996 / Accepted: 8 May 1996

Abstract. A new widely tunable source in the infrared for use in high-resolution spectroscopy and trace-gas detection is described. This spectroscopic source is based on Difference Frequency Generation (DFG) in gallium selenide (GaSe) and is continuously tunable in the 8.8–15.0 μm wavelength region. Such a DFG source operates at room temperature which makes it a useful alternative to a lead-salt diode-laser- based detection system that requires cryogenic temperatures and numerous individual diode lasers.

PACS: 7.65; 33.00; 42.60; 42.65; 42.80

There is considerable interest in developing convenient methods for selective and sensitive measurements of trace-gas concentrations. As virtually all fundamental vibrational modes of molecules and molecular ions lie in the 2–20 μm wavelength region, infrared (IR) spectroscopy provides a convenient and real-time method of detection for most gases. Hence, it is important to develop compact and reliable diode-laser-based sources in this spectral region.

Diode-based cw DFG spectroscopic sources have recently been demonstrated in the 3–5 μm region with periodically poled $LiNbO_3$ [1] and $AgGaS_2$ [2]. The present work aims to explore the feasibility of similar cw sources at wavelengths from 5 to 18 μm by mixing two visible lasers in the nonlinear crystal GaSe. Although the work described here uses two cw Ti:Sapphire lasers in order to explore the characteristics of the nonlinear optical material, it is envisioned that the pump lasers will ultimately be high-power visible/near-IR diode lasers to create a rugged portable IR source for gas monitoring.

Gallium selenide has been tested previously in pulsed DFG sources in the 4–19 μm region [3–8]. In addition, Vodopyanov et al. [9, 10] have measured the spontaneous parametric emission from GaSe pumped by a mode-locked Er:YAG (2.94 μm) laser. In all these experiments, pulsed lasers operating at wavelengths longer than 1 μm were used to generate the tunable IR radiation. In the only previous reported work with visible pumps, Abdullaev and co-workers used the pulsed output of a ruby laser and dye laser (715–750 nm) in a DFG source to generate pulsed radiation in the 9–18 μm region [11].

A good summary of the above experiments and many others can be found in the review article by Fernelius [12].

1 Experimental

The cw IR spectroscopic source, shown in Fig. 1, used the 20 W all-lines output of an argon ion laser to pump simultaneously two single-frequency cw Titanium:Sapphire ring lasers (Coherent Model 899-21 and 899-29). These lasers are actively frequency stabilized by locking to external etalons, and line widths in the near IR of 1 MHz are typical. Titanium:Sapphire lasers were used in this experiment because of their superior wavelength tuning, transverse-mode quality, and output power characteristics. The output from each laser was attenuated to < 300 mW using linearly variable filters to avoid optical damage of the GaSe crystal. The two beams were spatially overlapped by rotating the polarization of the pump beam orthogonal to the signal and combining them in a polarization cube to provide Type-I phase matching. Type-I phase matching was chosen in GaSe because the required external angle and walkoff effects are smaller than for Type II. The two beams are chopped and focussed with a 100 mm lens into a GaSe crystal 5 mm in length and 10 mm in diameter mounted on a rotation stage. The IR light generated in the GaSe crystal was collected and refocused with a single ZnSe lens onto a 1-mm-diameter liquid-nitrogen-cooled HgCdTe detector. A broadband antireflective-coated (3–13 μm) Ge flat is placed immediately in front of the detector to block the two pump beams. The output of the detector is monitored by a lock-in amplifier and recorded by a computer. A 50-cm-long absorption cell equipped with ZnSe windows was used for absorption experiments.

Dedicated to Prof. F. P. Schäfer on the occasion of his 65th birthday.

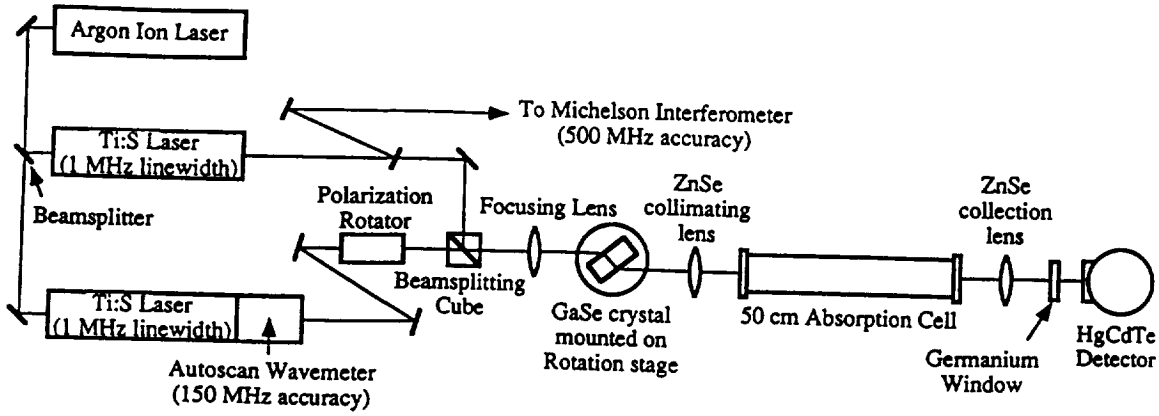

Fig. 1. Schematic diagram of a DFG spectroscopic source based on GaSe crystal.

To date, we have generated continuously tunable light from 8.8 to 15.0 μm by tuning the wavelength of the two pump lasers and the angle of the crystal. We are not fundamentally limited to this tuning range and could extend the range to 6 μm with larger crystal angles, but the present crystal mount restricts the GaSe external angle to less than 60°. We expected to be able to tune to the 18 μm absorption edge of the crystal but did not obtain significant IR power at wavelengths longer than 15 μm. Within the current 45–60° range of external angles it is possible to tune continuously over a 6.2 μm IR range using only a 25 nm tuning range of one of the visible/near-IR pump lasers.

The published Sellmeier coefficients [13–17] were found to be inadequate for accurately describing the combination of input wavelengths and crystal angles to generate IR light. The predicted pump wavelengths for a given external crystal angle and signal wavelength are too low by about 3% or 20–25 nm, which confirms the observations of the Abdullaev [16] and Bhar [18] groups. Abdullaev attributed these errors to insufficiently accurate determination of the ordinary index of refraction near the short-wavelength edge of the absorption band. The results of our systematic investigation for optimized phase-matched conditions are given in Fig. 2. We obtained each data point by fixing the crystal angle and the signal wavelength and by scanning the pump-laser wavelength. The results of one such scan is shown in Fig. 3. The noise in the trace is a result of limiting the input power of each beam to 25 mW average at the crystal to avoid possible thermal effects due to absorption. The phase-matching FWHM was found to be 0.706 nm (10.967 cm^{-1}) for a pump laser scan with the signal-laser wavelength fixed at 868.318 nm and the external crystal angle fixed at 51.2°.

We attempted to reoptimize the Sellmeier coefficients and found that the mathematical system was underdetermined. There were numerous solutions that fit our experimental data and some of these deviated from the previously published index-of-refraction dispersion relations. We, therefore, have chosen to present our data on predicting the GaSe-crystal external angle in a manner that makes no reference to the index of refraction so that no confusion results. The external crystal angle in degrees was fitted with a quadratic function of the pump

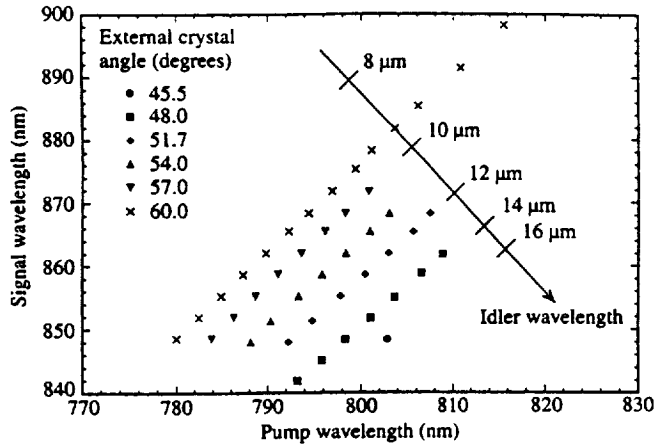

Fig. 2. Experimental phase-matching angles and wavelengths for a GaSe crystal in the 780–880 nm pumping region. Individual points represent combinations of external angles and pump wavelengths that optimize the IR DFG power. IR wavelengths are given by projecting the data points onto the diagonal axis labeled "idler wavelength"

wavelength (λ_p) in nanometers and the idler frequency (ν_i) in wave numbers:

$$\text{External angle} = 49.4 - 1.84 \times 10^{-5} \times \lambda_p^2 + 4.70 \times 10^{-5} \times \nu_i^2 - 4.37 \times 10^{-11} \times \lambda_p^2 \times \nu_i^2.$$

The fit to our 44 data points has a standard deviation of 0.12°. There is a high relative uncertainty in all the coefficients due to a linear dependence between variables which is not easily removed without transforming the observed variables of wavelength and frequency to non-intuitive units. The main source of experimental uncertainty was the measurement of the zero crystal angle. We were able to measure the back reflection at the polarization cube from normal incidence with respect to the GaSe crystal to within two millimeters which yielded an angular resolution of 0.2°. The uncertainty in the pump and signal wavelengths are several orders of magnitude below this angular uncertainty.

Under the plane-wave approximation, the phase-matching bandwidth is a simple function of the effective

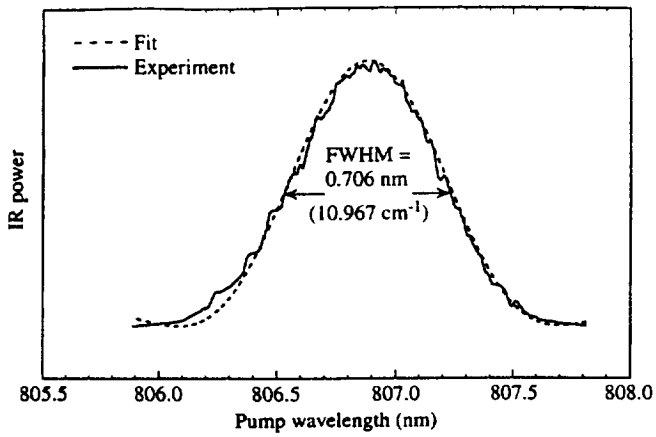

Fig. 3. Wavelength dependence of the IR power with fixed signal laser wavelength of 868.318 nm and fixed GaSe-crystal external angle of 51.2°

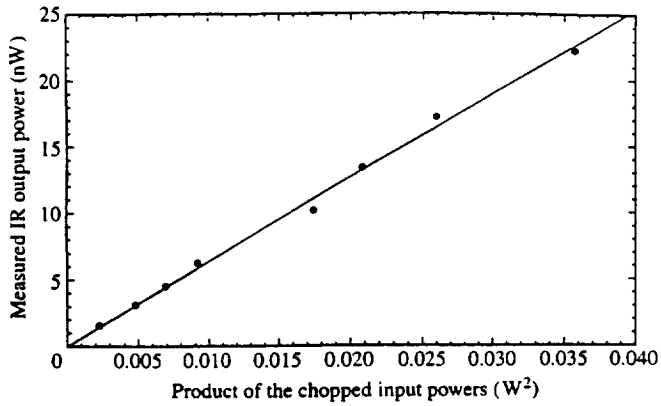

Fig. 4. IR DFG power vs the product of two input pump powers. The line is a least-squares fit to the data. The idler, pump, and signal wavelengths were 13.708 μm, 793.210 nm, and 841.925 nm, respectively, and the external angle was 48.3°

coherence length and the wave-vector mismatch. The output power can be regarded as proportional to $\mathrm{sinc}^2(\Delta k L_{\mathrm{eff}}/2)$. Assuming all three indices of refraction to be constant during a scan and $\Delta k = 0$ at the peak of the IR production, the Δk term can be approximated by (1):

$$\Delta k = 2\pi \times \left(\frac{1}{\lambda_p} - \frac{1}{\lambda_p^\circ}\right) \times (n_p - n_i), \tag{1}$$

where λ_p is the pump wavelength, λ_p° is the pump wavelength at which the output IR power is maximized, and n_p and n_i are the indices of refraction at the pump and idler wavelengths, respectively. In this fashion, only the difference between the indices of refraction are necessary to compute the wave-vector mismatch and is relatively insensitive to the choice of Sellmeier constants. The wave-vector mismatch is assumed to be equal to zero at the centroid of the experimental curve based on the observation that the curve does not exhibit the asymmetry shown in systems where the maximum output power and $\Delta k = 0$ do not coincide (see [19] for an example in the case of second-harmonic generation). The phase-matching bandwidth for unfocused and focused beams is found to be nearly identical so long as the beams are not in the overfocused condition. In this experiment, we deliberately underfocused the input beams by using an $f = 100$ mm lens instead of the $f = 66$ mm called for by theory. By fitting the observed spectrum with (1) where L_{eff} is the adjustable variable, it is possible to obtain agreement between theory and experiment. The value of L_{eff} determined from this fit is 2.9 mm – in agreement with [3] in which an L_{eff} value of 3.2 mm was obtained.

As a further test of our fitting, the L_{eff} parameter can be estimated by

$$L_{\mathrm{eff}} = \left(\frac{\lambda_p}{2\Delta n}\right),$$

where Δn is the change in index of the pump beam in turning the crystal to reduce the IR power to 40.5% of the peak value or when the accumulated phase error is equal to 180°. The value of Δn is calculated from the dispersion relations, and again it is found to be largely invariant with choice of Sellmeier coefficients. The resulting L_{eff} is 2.9 mm. Both our results imply that in this instance the coherence length is determining the power output and not the crystal length.

The effect of high input powers on the parametric conversion process was measured. Linearly variable neutral density filters were used to vary the input powers and the generated IR power plotted vs their product in Fig. 4. Thermal lensing can be a problem in the nonlinear optical conversion process – especially in the case of intense cw input beams [20]. This effect can cause the IR power to scale less than linearly with the product of the input powers but was not observed in GaSe as shown in Fig. 4. The experimental conversion efficiency derived from the slope of the fitted line in the figure is 28% of the calculated value obtained with a nonlinear coefficient $d_{22} = 54.4$ pm/V[16] at the specific wavelengths used in Fig. 4. The calculated power in the above comparison was corrected for Fresnel losses at all uncoated surfaces. Our best estimate of the detector calibration is ± 20%. A component of the discrepancy is the transverse distortion of the beam into an oval shape with non-normal incidence upon the GaSe crystal surface. This could be corrected with the use of a cylindrical focusing lens. A second explanation of the missing power is the possibility that the two input beams were focused at different longitudinal positions. We assumed that the lasers were operating to manufacturers' specifications and thus the foci were in the same location, but telescopes could be inserted in the beam path to verify this condition.

2 Spectroscopy of ethylene (C_2H_4)

The maximum mid-IR output measured by the present system is about 30 nW, which is sufficient for spectroscopic detection of many gases. It is feasible to design a mid-IR absorption-based gas sensor based on the mixing of two visible high-power laser diodes (in master oscillator-power amplifier geometries at the 0.5–1 W level)

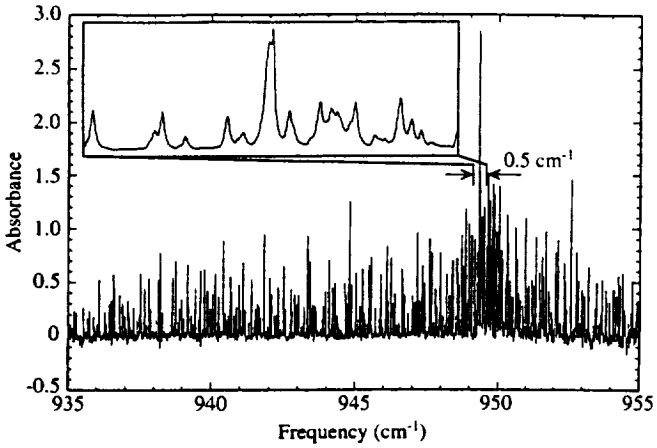

Fig. 5. A sample spectrum of the ethylene molecule near 945 cm^{-1} taken with a path length of 50 cm and a pressure of 20 mTorr. The inset is a 0.5 cm^{-1} blowup centered on the strongest absorption lines in the lower scan

in GaSe. This sensor would be capable of detecting numerous gases of interest in atmospheric monitoring – including but not limited to such species as hydrogen cyanide, acetylene, ethylene, ammonia, nitric acid, phosphine, ozone, methane, and nitrous oxide.

Ethylene is a very interesting biological molecule. It has been found to play a role in many developmental processes in plants: ripening of fruits, wilting of flowers, and the emergence from dormancy in some seeds and bulbs [21–23]. Environmental stresses, such as excessive water loss, mechanical damage, and lack of sufficient light, all stimulate the production of increased levels of C_2H_4 [24]. Ethylene concentrations have been monitored by gas chromatography and by photoacoustic detection using a carbon dioxide laser [25–27], though neither method is readily portable. Using difference frequency generation, it appears feasible to construct an ethylene sensor that is compact and battery driven.

In the 10-μm region, the absorption of ethylene gas is essentially due to the intense ν_7 C-type perpendicular IR band which presents a strong Q-branch near 950 cm^{-1}. The P and R branches cover the region from 800 to 1100 cm^{-1}. Much in the way of high-resolution spectroscopy has been conducted on this band [28–31]. Nearly all the lines in this region have been assigned and their positions known to sub-Doppler accuracy.

A 20 cm^{-1} scan of ethylene taken with the experimental apparatus is shown in Fig. 5. The inset spectrum is a blowup of 0.5 cm^{-1} centered around the most intense absorption lines. The total path length is 50 cm and the ethylene pressure is 20 mTorr. The scan was taken by fixing the signal laser at 868.750 nm, the external angle to 55.5°, and scanning the pump laser from 802.195 to 803.484 nm in 20 MHz steps. The lock-in amplifier was set to a 100 ms time constant with a 12 dB/octave rolloff. Because of etalon effects within the 3-mm-thick ZnSe flats used as windows for the absorption cell, the cell was pumped out and scanned to provide normalization.

3 Conclusion

In this work we have investigated the characteristics of using 780–900 nm pump sources to generate narrow bandwidth IR radiation which is continuously tunable from 8.8 to 15 μm in the nonlinear optical crystal GaSe. No thermal lensing effects are observed with chopped input powers of up to half-a-watt cw. It is now possible to predict the phase-matching angle in GaSe with an error that is less than the phase-matching angular bandwidth, thus assuring IR generation for a given combination of input wavelengths and calculated external angle. Such a tunable DFG IR source has the potential of becoming a valuable tool for environmental sensing, as demonstrated by the detection of ethylene.

Acknowledgements. The authors would like to thank K. Kato and D. Roberts for helpful discussions. This work was supported in part by the National Science Foundation and the Robert A. Welch Foundation. WCE is grateful to the Department of Defense for support in the form of an NDSEG fellowship. RSP and SW are grateful for support from the Department of Energy, Contract #DE-FG02-94ER81698, through Aerodyne Research.

References

1. K.P. Petrov, L. Goldberg, W.K. Burns, R.F. Curl, F.K. Tittel: Opt. Lett. **21**, 86 (1996)
2. K.P. Petrov, S. Waltman, U. Simon, R.F. Curl, F.K. Tittel, E.J. Dlugokensky, L. Hollberg: J. Appl. Phys. B **61**, 553 (1995)
3. A. Bianchi, A. Ferrario, M. Musci: Opt. Commun. **25**, 256 (1978)
4. A. Bianchi, M. Garbi: Opt. Commun. **30**, 122 (1979)
5. T. Dahinten, U. Plodereder, A. Seilmeier, K.L. Vodopyanov, K.R. Allakhverdiev, Z.A. Ibragimov: IEEE J. Quant. Electron. **29**, 2245 (1993)
6. J.L. Oudar, Ph. J. Kupecek, D.S. Chemla: Opt. Commun. **29**, 119 (1979)
7. Yu.A. Gusev, A.V. Kirpichnikov, S.N. Konoplin, S.I. Marennikov, P.V. Nikles, Yu.N. Polivanov, A.M. Prokhorov, A.D. Savel'ev, R. Sh. Sayakhov, V.V. Smirnov, V.P. Chebotaev: Sov. Tech. Phys. Lett. **6**, 541 (1980)
8. A. Suda, H. Tashiro: Digest of 16th Ann. Meeting Laser Soc. Japan, 53 (1996)
9. K.L. Vodopyanov, L.A. Kulevskii, V.G. Voevodin, A.I. Gribenyukov, K.R. Allakhverdiev, T.A. Kerimov: Opt. Commun. **83**, 322 (1991)
10. K.L. Vodopyanov: J. Opt. Soc. Am. B **10**, 1723 (1993)
11. G.B. Abdullaev, L.A. Kulevskii, P.V. Nikles, A.M. Prokhorov, A.D. Savel'ev, E.Yu. Salaev, V.V. Smirnov: Sov J. Quant. Electron. **6**, 88 (1976)
12. N.C. Fernelius: Prog. Crystal Growth and Charact. **28**, 275 (1994)
13. S. Adachi, Y. Shindo: J. Appl. Phys. **71**, 428 (1992)
14. G.B. Abdullaev, L.A. Kulevskii, A.M. Prokhorov, A.D. Savel'ev, E.Yu. Salaev, V.V. Smirnov: JETP Lett. **16**, 90 (1972)
15. N. Piccioli, R. Le Toullec, M. Mejatty, M. Balkanski: Appl. Opt. **16**, 1236 (1977)
16. G.B. Abdullaev, K.R. Allakhverdiev, L.A. Kulevskii, A.M. Prokhorov, E.Yu. Salaev, A.D. Savel'ev, V.V. Smirnov: Sov. J. Quant. Electron. **5**, 665 (1975)
17. K.L. Vodopyanov, L.A. Kulevskii: Opt. Commun. **118**, 375 (1995)
18. G.C. Bahr, S. Das, K.L. Vodopyanov: J. Appl. Phys. B **61**, 187 (1995)
19. G.D. Boyd, D.A. Kleinman: Appl. Phys. **39**, 3597 (1968)
20. C.E. Miller, W.C. Eckhoff, U. Simon, F.K. Tittel, R.F. Curl: SPIE **2145**, 282 (1994)

21. S.F. Yang, N.E. Hoffmann: Ann. Rev. Plant Physiol. **35**, 155 (1984)
22. F.B. Abeles: *Ethylene in Plant Biology* (Academic, London 1973) p. 302.
23. M.B. Jackson: In *Ethylene and Plant Development*, ed. by J.A. Roberts, G.A. Tucker (Butterworths, London 1985).
24. H. Mehlhorn, A.R. Wellburn: Nature **327**, 417 (1987)
25. L.B. Kreuzer, N.D. Kenyon, C.K.N. Patel: Science **177**, 347 (1972)
26. D. Bicanic, F. Harren, J. Reuss, E. Woltering, J. Snel, L.A.C.J. Voesenek, B. Zuidberg, H. Jalink, F. Bijnen, C.W.P.M. Blom, H. Sauren, M. Kooijman, L. van Hove, W. Tonk: In *Photoacoustic, Photothermal and Photochemical Processes in Gases*, ed. by P. Hess (Springer, New York 1989).
27. C. Brand, A. Winkler, P. Hess, A. Miklos, Z. Bozoki, J. Sneider: Appl. Opt. **34**, 3257 (1995)
28. W.L. Smith, I.M. Mills: J. Chem. Phys. **40**, 2095 (1964)
29. Ch. Lambeau, A. Fayt, J.L. Duncan, T. Nakagawa: J. Mol. Spectrosc. **81**, 227 (1980)
30. F. Herlemont, M. Lyszyk, J. Lemaire, Ch. Lambeau, A. Fayt: J. Mol. Spectrosc. **74**, 400 (1979)
31. I. Cauuet, J. Walrand, G. Blanquet, A. Valentin, L. Henry, Ch. Lambeau, M. de Vleeschouwer, A. Fayt: J. Mol. Spectrosc. **139**, 191 (1990)